

Electricfieldinduced Raman spectroscopy

David L. Andrews and Nick P. Blake

Citation: [The Journal of Chemical Physics](#) **88**, 6039 (1988); doi: 10.1063/1.454496

View online: <http://dx.doi.org/10.1063/1.454496>

View Table of Contents: <http://scitation.aip.org/content/aip/journal/jcp/88/10?ver=pdfcov>

Published by the [AIP Publishing](#)

Articles you may be interested in

[Resonant spectroscopy of electric-field-induced superlattices](#)

J. Appl. Phys. **90**, 2857 (2001); 10.1063/1.1392956

[Surface Fermi level pinning in epitaxial InSb studied by electricfieldinduced Raman scattering](#)

Appl. Phys. Lett. **63**, 349 (1993); 10.1063/1.110039

[Electricfieldinduced differential rotational Raman scattering](#)

J. Chem. Phys. **78**, 3393 (1983); 10.1063/1.445215

[Electricfieldinduced optical rectification in nitrobenzene](#)

Appl. Phys. Lett. **30**, 276 (1977); 10.1063/1.89365

[Electricfieldinduced transient spinflip Raman laser pulses in InSb](#)

Appl. Phys. Lett. **21**, 482 (1972); 10.1063/1.1654227



Electric-field-induced Raman spectroscopy

David L. Andrews and Nick P. Blake

School of Chemical Sciences, University of East Anglia, Norwich NR4 7TJ, England

(Received 7 October 1987; accepted 28 January 1988)

In this final paper of a series on electric-field-induced spectroscopy, the general theory of electro-optical effects in vibrational Raman spectroscopy is developed. It is demonstrated that the electrical polarization of a dipolar fluid can lead to appreciable intensity enhancement of certain lines in its Raman spectrum, and a modification of the polarization rules normally applicable to an isotropic medium. Exact intensity expressions are presented, and it is shown how the complete symmetry analysis of all Raman transitions can be accomplished with five intensity measurements, introducing new possibilities for species characterization close to electrode surfaces. It is also demonstrated that in intense electric fields a novel nonlinear electro-optical channel exists, whereby the electric field perturbs the stationary states of the system and gives rise to selection rules completely different to those which normally apply in Raman scattering. This can result in the appearance of entirely new lines in the spectrum. Detailed examination of the intensity expressions for the electro-optical route reveal that in this case five intensity measurements are required for a complete elucidation of the Raman spectrum.

I. INTRODUCTION

In recent years there has been much interest in the Raman spectroscopy of electrochemical systems.¹ Much of this interest has focused on the enhancement of Raman intensities associated with species adsorbed on electrode or other (usually metallic) surfaces. Surface-enhanced Raman spectroscopy (SERS) has been the subject of intense research effort, and as such has been extensively reviewed.^{2,3} The Raman effect has the merit of being amenable to study under potentiostatically controlled conditions,⁴ and the existence of very high local electric fields within the electrochemical double layer gives rise to many interesting phenomena.⁵ Comparatively little attention has been given to the effect of very high electric fields on the Raman spectrum of electrolytes or other fluid media, however.

As discussed in the first paper in this series⁶ (subsequently referred to as paper I), the application of a static electric field to a fluid can induce changes in the Raman spectrum via two distinct mechanisms. First, the field can give rise to an *electro-optical* interaction whereby it perturbs the molecular wave functions. This perturbation mixes the stationary states of the molecule and results in a modification of conventional selection rules.⁷ The electro-optical route thus gives rise to selection rules identical to those normally obtained in hyper-Raman spectroscopy,^{8,9} and can for example induce Raman activity in certain IR-inactive *ungerade* vibrations of centrosymmetric molecules.

Secondly, molecules with axial symmetry possessing a permanent dipole moment can interact with the static electric field to give an anisotropic distribution of molecular orientations within the fluid, which ultimately gives rise to changes in the intensity of Raman transitions. In pioneering studies ten years ago, Lippitsch *et al.*¹⁰⁻¹⁵ showed that Raman scattering experiments with axial molecules in the presence of pulsed electric fields of 10^6 – 10^8 V m⁻¹ produced intensity enhancements by a factor of 2–3. Indeed, there is

significant evidence for the orientation of *nonpolar* isotropic fluids, where large electric fields can induce appreciable dipole moments.^{10,16-18} The results obtained by Lippitsch *et al.* also suggested that judicious choice of solvent may increase the degree of enhancement. Solvents with large electric susceptibilities can introduce large local electric fields and so enhance the intensity of Raman transitions via both the electrically polarized and electro-optical channels.

In this, the final paper of a series on electric-field-induced spectroscopy, we adopt the theoretical methods detailed in paper I to investigate both types of electrochromic effect upon the vibrational Raman spectrum of a fluid. The intensity equations are calculated within a quantum electrodynamical framework, and the necessary rotational averaging is carried out by exact tensor methods derived in previous papers.^{19,20} Results are given for a variety of laser polarizations and beam geometries, and it is shown how to process the results to give the maximum information on the symmetry characteristics of the field-induced Raman transitions. Finally, an estimate of the experimental feasibility of observing these effects is discussed.

II. EFFECTS OF THE STATIC ELECTRIC FIELD ON RAMAN-ALLOWED TRANSITIONS IN POLAR MOLECULES

A. Quantum mechanics

The starting point for the theory of Raman processes is the Fermi Golden Rule, which gives the rate Γ for a transition from an initial vibrational state $|m\rangle$ to a final state $|n\rangle$ as

$$\Gamma_{m \rightarrow n} = \frac{2\pi\rho_f}{\hbar} |M_{nm}|^2. \quad (2.1)$$

Here ρ_f is the density of final states for the scattered radiation, and M_{nm} is the quantum mechanical matrix element for the process. In the presence of the static electric field, this

matrix element can be approximated by considering only the dominant second-order ($E1 \times E1$) and third-order ($E1 \times E1 \times E1$) terms in the perturbation expansion, [cf. Eq. (2.7) of paper I], i.e.,

$$M_{nm} = \frac{\hbar c (n k k')^{1/2}}{2\epsilon_0 V} (\alpha_{ij} e_i \bar{e}_j' + T_{ijk} e_i \bar{e}_j' E_k), \quad (2.2)$$

where α_{ij} is the normal Raman scattering tensor and T_{ijk} an electro-optical Raman scattering tensor derived in Sec. III: \mathbf{e} is the polarization vector of the incident laser beam with frequency $\omega = ck$, \mathbf{e}' is that of the scattered radiation with frequency $\omega' = ck'$, and \mathbf{E} is the static electric field. The time-averaged photon density of the laser radiation is n/V .

In this section, we examine the effect of the applied field upon ($E1 \times E1$)-allowed transitions in axially symmetric molecules possessing a permanent electric dipole moment, where the first term in the matrix element (2.2) dominates. Applying the Born–Oppenheimer approximation and neglecting the vibrational contribution to vibronic energy differences^{21,22} leads to the result

$$M_{nm} = -\{\hbar c/2\epsilon_0 V\} [n k k']^{1/2} \times \langle \chi_{0m} | \sum_r \frac{(\mu^{mr} \cdot \mathbf{e} \mu^{r0} \cdot \bar{\mathbf{e}}')}{E_{r0} - \hbar ck} + \frac{(\mu^{mr} \cdot \bar{\mathbf{e}}' \mu^{r0} \cdot \mathbf{e})}{E_{r0} + \hbar ck} | \chi_{0m} \rangle \\ = -\{\hbar c/2\epsilon_0 V\} [n k k']^{1/2} e_i \bar{e}_j' \langle \chi_{0n} | \alpha_{ij}^{00} | \chi_{0m} \rangle. \quad (2.3)$$

Here $|\chi_{0m}\rangle$ is the vibrational wave function for the m th level of a vibrational mode in the zeroth electronic state: α_{ij}^{00} is the index-symmetric frequency-dependent dynamic polarizability tensor. Since we deal only with off-resonance Raman scattering in this paper, damping of the virtual intermediate states for the process is ignored and α_{ij} is taken to be real. Using Eq. (2.1) and reexpressing the result in terms of the incident laser irradiance I gives the following expression for the radiant intensity of Raman scattering:

$$I(\mathbf{k}') = (Ik'^4/16\pi^2\epsilon_0^2) e_i \bar{e}_j' \bar{e}_k e_l' \alpha_{ij}^{0n,0m} \alpha_{kl}^{0n,0m}, \quad (2.4)$$

where

$$\alpha_{ij}^{0n,0m} = \langle \chi_{0n} | \alpha_{ij}^{00} | \chi_{0m} \rangle. \quad (2.5)$$

Expanding Eq. (2.5) as a Taylor series about the molecular equilibrium configuration, in terms of the vibrational mode coordinates Q , the dominant term for Raman scattering is nonvanishing only when $n = m \pm 1$. Examination of the Hermite polynomials shows that for even m , $|\chi_{0m}\rangle$ spans the totally symmetric irreducible representation, and when m is odd it transforms according to the symmetry of Q itself. The selection rule $n = m \pm 1$ thus dictates that the Raman tensor must transform under the same representation as the vibrational mode for the transition to be allowed.

Equation (2.4) gives the scattered Raman intensity for the transition $|n\rangle \leftarrow |m\rangle$ in the solid angle around \mathbf{k}' , and as it stands the equation is applicable to crystals or molecules with fixed orientation. However when the molecules do not have fixed orientation with respect to the laser radiation the result has to be rotationally averaged.

B. Rotational averaging

The intensity of scattered radiation for a fluid containing molecules of axial symmetry in a static electric field is given by the Boltzmann-weighted rotational average of Eq. (2.4). Using the procedure expounded in Sec. III of paper I, we obtain from Eqs. (3.9) and (3.10) of that paper the following result:

$$I(\mathbf{k}') = (Ik'^4/16\pi^2\epsilon_0^2) \times [e_i \bar{e}_j' \bar{e}_k e_l' \alpha_{\lambda\mu}^{nm} \alpha_{\nu o}^{nm} I_{ijkl,\lambda\mu\nu o}^{(4)\varphi} (-i\gamma, \hat{\mathbf{E}}, \hat{\boldsymbol{\mu}}^{00})], \quad (2.6)$$

where $I_{ijkl,\lambda\mu\nu o}^{(4)\varphi} (-i\gamma, \hat{\mathbf{E}}, \hat{\boldsymbol{\mu}}^{00})$ represents the weighted fourth rank tensor average, expressible as

$$I_{ijkl,\lambda\mu\nu o}^{(4)\varphi} = \sum_{j=0}^4 I_{ijkl,\lambda\mu\nu o}^{(4;j)\varphi}. \quad (2.7)$$

It can be shown that the (λ, μ) and (ν, o) index symmetry results in odd- j contributions to the rotational average vanishing when linearly polarized light is used, and consequently Eq. (2.7) reduces to a sum over the even j ,

$$I_{ijkl,\lambda\mu\nu o}^{(4)\varphi} = \sum_{k=0}^2 I_{ijkl,\lambda\mu\nu o}^{(4;2k)\varphi}. \quad (2.8)$$

By applying the explicit results for the weighted average given by Andrews and Harlow²⁰ we thus obtain a result which can be expressed in terms of a sum of reduced spherical Bessel functions of orders 0, 2, and 4:

$$I = K [A + j_2'(-i\gamma)B + j_4'(-i\gamma)C], \quad (2.9)$$

where $K = (Ik'^4/16\pi^2\epsilon_0^2)$, and the rate contributors A , B , and C are given explicitly in Appendix A. As before γ is defined as $\mu^{00}E_{\text{mol}}/kT$ and $j_n'(-i\gamma)$ are the reduced Bessel functions defined by the relation

$$j_n'(-i\gamma) = j_n(-i\gamma)/j_0(-i\gamma). \quad (2.10)$$

The expansions of these functions in their high- and low-temperature (low field and high field) limits are given in Table I of paper I.

At room temperature and with external electric field strengths of less than 10^6 V m^{-1} we generally have $\gamma \ll 1$, and the reduced spherical Bessel functions can be approximated by the relation $j_n'(-i\gamma) \approx (-i\gamma)^n/(2n+1)!!$. Then Eq. (2.9) is reduced to a quartic equation in γ :

$$I = K(A - B\gamma^2/15 + C\gamma^4/945). \quad (2.11)$$

In this form it is evident that in the low-field limit we have $\lim_{\gamma \rightarrow 0} I = KA$. The γ -independent term, KA , corresponds to the conventional result for the intensity of Raman scattering from an isotropic system.²¹ At electric field strengths of 10^8 V m^{-1} or above, and at realistic liquid-state temperatures, γ can exceed unity, and under these conditions Eq. (2.9) should be employed. In the case of nitrobenzene, for example, at 300 K and under an external field of 10^8 V m^{-1} , the fluid is significantly polarized by the field and, as discussed in paper I, leads to a value for γ of about 4. The coefficient of the B term in Eq. (2.9) is then approximately three times as large as the coefficient of the isotropic term. As Lippitsch *et al.* have discovered,^{10–14} nitrobenzene in fields of comparable magnitude gives experimentally observed intensity en-

hancement factors of 2–3. Thus it seems likely that the phenomenon is a result of molecular alignment with the electric field.

We note in passing that in the case of resonance-Raman spectroscopy, the scattering tensor does not have index symmetry (because vibrational energy differences cannot be neglected),²² and the rotational average given in Eq. (2.9) is therefore incomplete. The correct rotational average is then given by the Raman analog of Eq. (3.9) of the second paper in this series,²³ subsequently referred to as paper II. However a note of caution is added here. Under resonance conditions, the electric field associated with the laser light itself can produce very sizable induced dipole moments and thus lead to a different kind of molecular orientation. The theory is described in detail in a forthcoming paper.¹⁷

At this stage, the intensity equations are expressed in terms of the reducible tensor $\alpha_{\lambda\mu}^{nm}$, and represent the Raman analogs of the results given in Appendix A of paper II. In order to facilitate symmetry treatments it is helpful to cast the intensity equations in terms of irreducible tensors. The necessary rank-2 irreducible parts of the Raman scattering tensor are given by Eqs. (4.1)–(4.4) of paper I; in the off-resonant case where the tensor is index-symmetric, the weight-1 part obviously vanishes. When the incident light is linearly polarized we obtain the general intensity equation given in Eqs. (A1)–(A3) of Appendix A at the end of this paper. In the next section we show how these equations can be used to facilitate the vibrational symmetry analysis of spectra obtained from samples which are significantly ordered by the electric field.

C. Polarization analysis

In this section it is demonstrated how five intensity measurements under different polarization conditions are sufficient for the assignment of each line in the Raman spectrum to one of the three possible symmetry classes. The beam geometry required is illustrated in Fig. 1. There are two directions for application of the static electric field; E_1 represents a field applied perpendicularly to the scattering plane, $(\mathbf{k}, \mathbf{k}')$, and E_2 a field whose direction vector lies in the plane, as shown in Fig. 1. In what follows $I(n, \theta)(x \rightarrow y)$ is used to denote the intensity of the scattered light polarization component y when the laser beam is polarized in the x direction; the symbols \perp and \parallel represent polarizations perpendicular to, and in the scattering plane, respectively. The label n denotes the direction of the static field, and θ is the angle, mea-

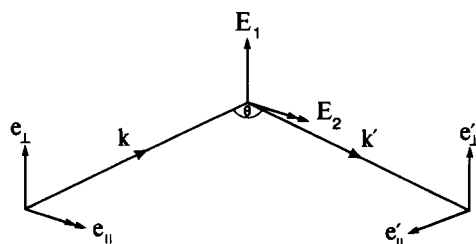


FIG. 1. Beam geometries for electric-field-induced Raman spectroscopy in polarized media.

sured in degrees, between the incident beam and the direction of observation, i.e., $\cos^{-1}(-\mathbf{k} \cdot \mathbf{k}')$. The beam geometries we describe have been chosen to facilitate the option of employing several electronically gated detectors.

In order to characterize the symmetry of any transition it is necessary to perform five intensity measurements; a suitable set is $I^{(1,90)}(\parallel \rightarrow \parallel)$, $I^{(2,90)}(\parallel \rightarrow \parallel)$, $I^{(2,90)}(\perp \rightarrow \perp)$, $I^{(1,35.3)}(\parallel \rightarrow \parallel)$, and $I^{(2,35.3)}(\parallel \rightarrow \parallel)$. [35.3° is the angle whose cosine is $\sqrt{(2/3)}$.] It is possible to form two linear combinations from these such that just one real, positive molecular parameter from each tensor weight contributes. These are defined as

$$I_1 = [I^{(1,90)}(\parallel \rightarrow \parallel) + (7/4)I^{(2,90)}(\parallel \rightarrow \parallel) + I^{(2,90)}(\perp \rightarrow \perp) + (3/4)I^{(1,35.3)}(\parallel \rightarrow \parallel)] \\ = [(1/2 + (2j_2'(-i\gamma)/21))\alpha_{(\lambda\mu)}^{(0)}\alpha_{(\lambda\mu)}^{(0)} + (2/5)\alpha_{(\lambda\mu)}^{(2)}\alpha_{(\lambda\mu)}^{(2)}], \quad (2.12)$$

$$I_2 = [I^{(1,90)}(\parallel \rightarrow \parallel) + (7/2)I^{(2,90)}(\parallel \rightarrow \parallel) + 3I^{(1,35.3)}(\parallel \rightarrow \parallel) + (3/2)I^{(2,35.3)}(\parallel \rightarrow \parallel)] \\ = [\alpha_{(\lambda\mu)}^{(0)}\alpha_{(\lambda\mu)}^{(0)} + (4/5)\alpha_{(\lambda\mu)}^{(2)}\alpha_{(\lambda\mu)}^{(2)}]. \quad (2.13)$$

Explicit equations for these intensities are given in Appendix B. The ratio of the above intensity expressions defines a polarization ratio η whose value for a given transition is sufficient to classify the symmetry class:

$$\eta = I_1/I_2 \\ = \frac{\sigma\alpha_{(\lambda\mu)}^{(0)}\alpha_{(\lambda\mu)}^{(0)} + (2/5)\alpha_{(\lambda\mu)}^{(2)}\alpha_{(\lambda\mu)}^{(2)}}{\alpha_{(\lambda\mu)}^{(0)}\alpha_{(\lambda\mu)}^{(0)} + (4/5)\alpha_{(\lambda\mu)}^{(2)}\alpha_{(\lambda\mu)}^{(2)}}, \quad (2.14)$$

where

$$\sigma = [\frac{1}{2} + (2j_2'(-i\gamma)/21)]. \quad (2.15)$$

By first calculating the value of γ , as defined in terms of μ^{00} , E , and T , then use of Eqs. (2.14) and (2.15) in conjunction with tables of the spherical Bessel functions enables σ to be evaluated for any particular experiment. Note that E must be the static electric field strength *within the fluid* as given by Eq. (3.2) of paper I. In passing we note that where ionic species are present within the fluid, it is necessary to take account of diffusion processes at the electrodes which further affect the local electric field; the appropriate formula is given in the discussion section. Alternatively, an experimental procedure can be employed to calculate the local field. For example the local electric field close to metal surfaces can be calculated from reflectivity measurements.⁵

For experiments involving low electric field strengths where $\gamma \ll 1$, the value of $j_2'(-i\gamma)$ will be very small indeed. The analytical utility of the calculation for such a case is clearly minimal. However for large field strengths where $\gamma > 1$, η can be used like the familiar Raman depolarization ratio ρ for the characterization of vibrational symmetry. A value for η can be calculated for each line in the Raman spectrum. A pure weight-2 transition produces the result $\eta = 1/2$; otherwise η must lie in the range $(1/2, \sigma)$. The

limiting value $\eta = \sigma$ cannot be attained since it corresponds to a pure weight-0 transition; however there are no vibrations of this symmetry type in polar molecules, since in the axial point groups to which they belong the irreducible representation of the weight-0 tensor is always spanned by weight-2 tensor components. As a consequence the orientation of polar molecules by the applied field does not generally produce new lines in the Raman spectrum (cf. Sec. III). This is nonetheless possible with electric-field-induced resonance-Raman scattering, where the configuration $I^{(90)}(\perp \rightarrow \perp)$ provides access to pure weight-1 transitions on application of the field. This behavior can only be observed in molecules belonging to the point groups C_{nv} ($n \geq 3$): the detailed rate equations are the Raman analogs of the results presented in paper II.

III. OPTICALLY FORBIDDEN TRANSITIONS

A. Construction of the electro-optical Raman scattering tensor

When a vibrational Raman transition is forbidden in the $(E \perp E)$ approximation, the first term in Eq. (2.2) vanishes and the leading contribution to the matrix element involves the third rank electro-optical tensor T_{ijk} ;

$$M_{nm} = e_i \bar{e}_j' E_k T_{ijk}. \quad (3.1)$$

Under these condition the transition rate $\Gamma_{m \rightarrow n}$ is

$$\Gamma_{m \rightarrow n} = (2\pi\rho_f/\hbar) e_i \bar{e}_j' E_k \bar{e}_l' e_m' E_n T_{ijk} \bar{T}_{lmn}. \quad (3.2)$$

To proceed further with the calculation of the rate it is necessary to derive the form of T_{ijk} . This can be calculated directly using the time-dependent perturbation treatment outlined in paper II. T_{ijk} has three contributions corresponding to the six possible time-orderings given in Fig. 2. These contributions are:

$$M_{nm}(a) = \sum_{s,r} \{ \hbar c / 2V\epsilon_0 \} [kk'n]^{1/2} e_i \bar{e}_j' E_k \times \left[\frac{\mu_i^{ns} \mu_j^{sr} \mu_k^{rm}}{E_{rm} (E_{sm} - \hbar\omega)} + \frac{\mu_j^{ns} \mu_i^{sr} \mu_k^{rm}}{E_{rm} (E_{sm} + \hbar\omega')} \right], \quad (3.3)$$

$$M_{nm}(b) = \sum_{r,s} \{ \hbar c / 2V\epsilon_0 \} [kk'n]^{1/2} e_i \bar{e}_j' E_k \times \left[\frac{\mu_i^{ns} \mu_k^{sr} \mu_j^{rm}}{(E_{rm} - \hbar\omega)(E_{sm} - \hbar\omega)} + \frac{\mu_j^{ns} \mu_k^{sr} \mu_i^{rm}}{(E_{rm} + \hbar\omega')(E_{sm} + \hbar\omega')} \right], \quad (3.4)$$

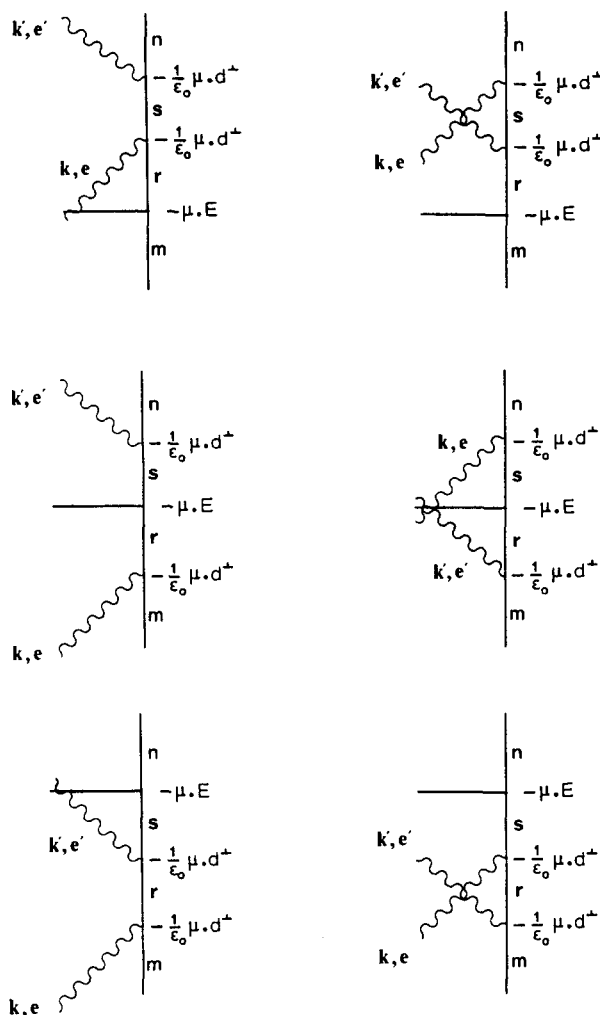


FIG. 2. Time-ordered diagrams for electro-optical Raman scattering.

$$M_{nm}(c) = \sum_{s,r} \{ \hbar c / 2V\epsilon_0 \} [kk'n]^{1/2} e_i \bar{e}_j' E_k \times \left[\frac{\mu_k^{ns} \mu_i^{sr} \mu_j^{rm}}{(E_{rm} - \hbar\omega)(E_{sm} - \hbar(\omega - \omega'))} + \frac{\mu_k^{ns} \mu_j^{sr} \mu_i^{rm}}{(E_{rm} + \hbar\omega')(E_{sm} - \hbar(\omega - \omega'))} \right], \quad (3.5)$$

where

$$M_{nm} = M_{nm}(a) + M_{nm}(b) + M_{nm}(c). \quad (3.6)$$

In order to make the expression for the rate less cumbersome, we define the third rank electro-optical Raman scattering tensor T_{ijk} as

$$T_{ijk} = \sum_{r,s} \left[\frac{\mu_i^{ns} \mu_j^{sr} \mu_k^{rm}}{E_{rm} (E_{sm} - \hbar\omega)} + \frac{\mu_j^{ns} \mu_i^{sr} \mu_k^{rm}}{E_{rm} (E_{sm} + \hbar\omega')} + \frac{\mu_i^{ns} \mu_k^{sr} \mu_j^{rm}}{(E_{rm} - \hbar\omega)(E_{sm} - \hbar\omega)} + \frac{\mu_j^{ns} \mu_k^{sr} \mu_i^{rm}}{(E_{rm} + \hbar\omega')(E_{sm} + \hbar\omega')} \right. \\ \left. + \frac{\mu_k^{ns} \mu_i^{sr} \mu_j^{rm}}{(E_{rm} - \hbar\omega)[E_{sm} - \hbar(\omega - \omega')]} + \frac{\mu_k^{ns} \mu_j^{sr} \mu_i^{rm}}{(E_{rm} + \hbar\omega')[E_{sm} - \hbar(\omega - \omega')]} \right]. \quad (3.7)$$

This real tensor describes at quantum level the concerted action of three electro-dynamical events. The static electric field behaves as a photon of zero frequency, and the electro-optical Raman scattering tensor is thus equivalent to a low-frequency limit ($\hbar\omega_2 \rightarrow 0$) of the hyper-Raman scattering tensor. It is therefore not surprising that electro-optical Raman scattering has identical selection rules to hyper-Raman scattering, as will become apparent.

The formula for the tensor T_{ijk} given above can be sim-

plified appreciably, and reexpressed in a form which facilitates a subsequent symmetry analysis of vibrational Raman transitions. First we reformulate T_{ijk} solely in terms of the incident frequency ω using the following relations:

$$\begin{aligned} E_{nm} &= \hbar(\omega - \omega'), \\ E_{ms} &= E_{ns} - E_{nm}, \\ E_{mr} &= E_{nr} - E_{nm}, \end{aligned} \quad (3.8)$$

so that we have

$$\begin{aligned} T_{ijk} = \sum_{r,s} & \left[\frac{\mu_i^{ns} \mu_j^{sr} \mu_k^{rm}}{E_{rm} (E_{sm} - \hbar\omega)} + \frac{\mu_j^{ns} \mu_i^{sr} \mu_k^{rm}}{E_{rm} (E_{sn} + \hbar\omega)} + \frac{\mu_i^{ns} \mu_k^{sr} \mu_j^{rm}}{(E_{rm} - \hbar\omega) (E_{sm} - \hbar\omega)} + \frac{\mu_j^{ns} \mu_k^{sr} \mu_i^{rm}}{(E_{rm} + \hbar\omega) (E_{sn} + \hbar\omega)} \right. \\ & \left. + \frac{\mu_k^{ns} \mu_i^{sr} \mu_j^{rm}}{(E_{rm} - \hbar\omega) E_{sn}} + \frac{\mu_k^{ns} \mu_j^{sr} \mu_i^{rm}}{(E_{rm} + \hbar\omega) E_{sn}} \right]. \end{aligned} \quad (3.9)$$

The tensor can be further simplified by invoking the usual Born–Oppenheimer and Placzek approximations,²⁴ leading to the following result for the matrix element:

$$\begin{aligned} M_{nm} &= \{\hbar c/2V\epsilon_0\} [kk'n]^{1/2} e_i \bar{e}'_j E_k \langle \chi_{0n} | \sum_{r,s} \left[\frac{\mu_i^{0s} \mu_j^{sr} \mu_k^{r0}}{E_{r0} (E_{s0} - \hbar\omega)} + \frac{\mu_j^{0s} \mu_i^{sr} \mu_k^{r0}}{E_{r0} (E_{s0} + \hbar\omega)} + \frac{\mu_i^{0s} \mu_k^{sr} \mu_j^{r0}}{(E_{r0} - \hbar\omega) (E_{s0} - \hbar\omega)} \right. \right. \\ & \left. \left. + \frac{\mu_j^{0s} \mu_k^{sr} \mu_i^{r0}}{(E_{r0} + \hbar\omega) (E_{s0} + \hbar\omega)} + \frac{\mu_k^{0s} \mu_i^{sr} \mu_j^{r0}}{(E_{r0} - \hbar\omega) E_{s0}} + \frac{\mu_k^{0s} \mu_j^{sr} \mu_i^{r0}}{(E_{r0} + \hbar\omega) E_{s0}} \right] | \chi_{0m} \rangle \right. \\ & \left. = \{\hbar c/2V\epsilon_0\} [kk'n]^{1/2} e_i \bar{e}'_j E_k \langle \chi_{0n} | \alpha_{ijk}^{00} | \chi_{0m} \rangle. \end{aligned} \quad (3.10)$$

In this form it is possible to prove that α_{ijk}^{00} is symmetric in its first two indices. This is easily demonstrated by interchanging the arbitrary labels r and s for the virtual intermediate states in the above expression, and using the fact that the transition dipoles are real; on rearranging the terms the result is equivalent to the exchange of the i and j indices in the original expression. The index symmetry arises as a result of the Placzek approximations. This has important ramifications for the later symmetry analysis, since it means that T_{ijk} has no weight-0 representation and only two weight-1 and one weight-2 representations.⁶

The rate, $\Gamma_{m \rightarrow n}$, for the transition $m \rightarrow n$ via the electro-optical route is obtained by inserting Eq. (3.10) into the Fermi Golden Rule expression of Eq. (2.1). Expressing the result in terms of the radiant intensity of Raman scattering, we obtain the result

$$I(k') = K e_i \bar{e}'_j E_k \bar{e}_m \bar{E}_n T_{ijk} T_{lmn}. \quad (3.13)$$

The required rotational average is effected using the tensor averaging method outlined in paper I. An isotropic rotational average is appropriate since it is mainly in molecules belonging to one of the nonaxial point groups that we find ($E1 \times E1 \times E1$) (electro-optically) allowed transitions which are not also ($E1 \times E1$) (optically) allowed. The general result given in Eq. (4.17) of paper I can be simplified by taking consideration of the real and index-symmetric nature of the molecular tensor. As with optically allowed Raman scattering the selection rule $n = m \pm 1$ still dominates, and

therefore some component of the electro-optical Raman scattering tensor must transform under the same representation as the Raman-active vibration [cf. Eq. (5.2) of paper I].

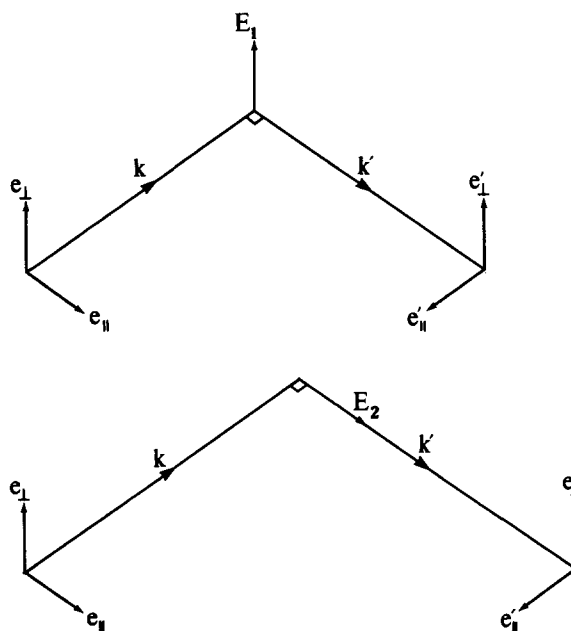


FIG. 3. Beam geometries for electro-optical Raman spectroscopy: (a) with the electric field perpendicular to the scattering plane; (b) with the electric field directed towards the detection optics.

B. Polarization analysis

While the result represented by Eq. (4.17) of paper I is hardly in a form amenable to direct experimental verification, its application does enable very useful information regarding the symmetry of the final state to be obtained by a fairly simple polarization analysis. By studying how the intensities of the Stokes (or anti-Stokes) lines vary with the relative polarizations of the incident and scattered light, it should be possible to unambiguously assign all the observed Raman transitions to a definite symmetry class. Under non-resonant conditions there is a set of five linearly independent irreducible tensor inner products that needs to be evaluated if the symmetry of any transition is to be determined. This requires the experimental determination of five spectra with linearly independent intensity equations. Detailed analysis of the results for the case of plane polarized light reveals that there is no suitable set of measurements whose intensities

have the required linear independence; we therefore concentrate on the case of circular polarization.

A total of five intensity measurements is required using a 90° scattering geometry. Three of the intensity measurements are made with \mathbf{k}' perpendicular to \mathbf{E} , henceforth referred to as beam geometry 1 [see Fig. 3(a)]. These intensities are denoted as $I^1(c \rightarrow c)$, $I^1(c \rightarrow \parallel)$, and $I^1(c \rightarrow \perp)$. $I^1(c \rightarrow c)$ refers to the intensity of scattered light with the same helicity as the incident light. $I^1(c \rightarrow \parallel)$ is the intensity of scattered light linearly polarized within the scattering plane, and $I^1(c \rightarrow \perp)$ is the intensity of scattered light polarized perpendicular to this plane. The other two intensities are made with \mathbf{k}' parallel to \mathbf{E} , henceforth referred to as beam geometry 2 [see Fig. 3(b)]. These intensities are $I^2(c \rightarrow c)$ and $I^2(c \rightarrow \perp)$. The intensity equations obtained on resolving Eq. (4.17) of Ref. 1 into its linearly independent components for each geometry are given in Appendix C for arbitrary scattering angle. The five required intensities have the explicit form shown below:

$$I^1(c \rightarrow c) = \frac{1}{2}K \left[-21T_{(\lambda\mu)\nu}^{(1\alpha)} T_{(\lambda\mu)\nu}^{(1\alpha)} - 56T_{(\lambda\mu)\nu}^{(1\alpha)} T_{(\lambda\mu)\nu}^{(1\beta,1\gamma)} + 259T_{(\lambda\mu)\nu}^{(1\beta,1\gamma)} T_{(\lambda\mu)\nu}^{(1\beta,1\gamma)} + 259T_{(\lambda\mu)\nu}^{(2)} T_{(\lambda\mu)\nu}^{(2)} + 66T_{(\lambda\mu)\nu}^{(3)} T_{(\lambda\mu)\nu}^{(3)} \right], \quad (3.14)$$

$$I^1(c \rightarrow \parallel) = \frac{1}{2}K \left[7T_{(\lambda\mu)\nu}^{(1\alpha)} T_{(\lambda\mu)\nu}^{(1\alpha)} + 168T_{(\lambda\mu)\nu}^{(1\alpha)} T_{(\lambda\mu)\nu}^{(1\beta,1\gamma)} + 343T_{(\lambda\mu)\nu}^{(1\beta,1\gamma)} T_{(\lambda\mu)\nu}^{(1\beta,1\gamma)} + 476T_{(\lambda\mu)\nu}^{(2)} T_{(\lambda\mu)\nu}^{(2)} + 52T_{(\lambda\mu)\nu}^{(3)} T_{(\lambda\mu)\nu}^{(3)} \right], \quad (3.15)$$

$$I^1(c \rightarrow \perp) = \frac{1}{2}K \left[35T_{(\lambda\mu)\nu}^{(1\alpha)} T_{(\lambda\mu)\nu}^{(1\alpha)} - 280T_{(\lambda\mu)\nu}^{(1\alpha)} T_{(\lambda\mu)\nu}^{(1\beta,1\gamma)} + 175T_{(\lambda\mu)\nu}^{(1\beta,1\gamma)} T_{(\lambda\mu)\nu}^{(1\beta,1\gamma)} + 42T_{(\lambda\mu)\nu}^{(2)} T_{(\lambda\mu)\nu}^{(2)} + 80T_{(\lambda\mu)\nu}^{(3)} T_{(\lambda\mu)\nu}^{(3)} \right], \quad (3.16)$$

$$I^2(c \rightarrow c) = \frac{1}{4}K \left[126T_{(\lambda\mu)\nu}^{(1\alpha)} T_{(\lambda\mu)\nu}^{(1\alpha)} + 784T_{(\lambda\mu)\nu}^{(1\alpha)} T_{(\lambda\mu)\nu}^{(1\beta,1\gamma)} + 651T_{(\lambda\mu)\nu}^{(1\beta,1\gamma)} T_{(\lambda\mu)\nu}^{(1\beta,1\gamma)} + 770T_{(\lambda\mu)\nu}^{(2)} T_{(\lambda\mu)\nu}^{(2)} + 116T_{(\lambda\mu)\nu}^{(3)} T_{(\lambda\mu)\nu}^{(3)} \right], \quad (3.17)$$

$$I^2(c \rightarrow \perp) = \frac{1}{4}K \left[119T_{(\lambda\mu)\nu}^{(1\alpha)} T_{(\lambda\mu)\nu}^{(1\alpha)} + 616T_{(\lambda\mu)\nu}^{(1\alpha)} T_{(\lambda\mu)\nu}^{(1\beta,1\gamma)} + 301T_{(\lambda\mu)\nu}^{(1\beta,1\gamma)} T_{(\lambda\mu)\nu}^{(1\beta,1\gamma)} + 294T_{(\lambda\mu)\nu}^{(2)} T_{(\lambda\mu)\nu}^{(2)} + 64T_{(\lambda\mu)\nu}^{(3)} T_{(\lambda\mu)\nu}^{(3)} \right]. \quad (3.18)$$

Equations (3.14)–(3.18) can be used to define two polarization ratios sufficient to elucidate the symmetry of each line in the spectrum. Using the four intensity expressions

$$\Phi = I^1(c \rightarrow \parallel) + I^1(c \rightarrow \perp) - 2I^1(c \rightarrow c), \quad (3.19)$$

$$\Gamma = (1/16)\{45I^1(c \rightarrow \parallel) - 41I^1(c \rightarrow c) - 16I^2(c \rightarrow \perp)\}, \quad (3.20)$$

$$\xi = \{8I^1(c \rightarrow c) + (6/5)I^1(c \rightarrow \perp) + 2I^2(c \rightarrow c)\}, \quad (3.21)$$

$$\xi = (5/2)I^1(c \rightarrow c) + (3/2)I^2(c \rightarrow \perp) - 2I^2(c \rightarrow c), \quad (3.22)$$

we define

$$\delta_1 = \Phi/\Gamma, \quad (3.23)$$

$$\delta_2 = \xi/\xi, \quad (3.24)$$

leading to the results

$$\delta_1 = \frac{1344T_{(\lambda\mu)\nu}^{(1\alpha)} T_{(\lambda\mu)\nu}^{(1\alpha)}}{720T_{(\lambda\mu)\nu}^{(1\alpha)} T_{(\lambda\mu)\nu}^{(1\alpha)} + 6097T_{(\lambda\mu)\nu}^{(2)} T_{(\lambda\mu)\nu}^{(2)} + 1397T_{(\lambda\mu)\nu}^{(3)} T_{(\lambda\mu)\nu}^{(3)}}, \quad (3.25)$$

$$\delta_2 = \frac{5866T_{(\lambda\mu)\nu}^{(1\beta,1\gamma)} T_{(\lambda\mu)\nu}^{(1\beta,1\gamma)} + 5785T_{(\lambda\mu)\nu}^{(2)} T_{(\lambda\mu)\nu}^{(2)} + 1480T_{(\lambda\mu)\nu}^{(3)} T_{(\lambda\mu)\nu}^{(3)}}{896T_{(\lambda\mu)\nu}^{(1\beta,1\gamma)} T_{(\lambda\mu)\nu}^{(1\beta,1\gamma)} + 637T_{(\lambda\mu)\nu}^{(2)} T_{(\lambda\mu)\nu}^{(2)} + 290T_{(\lambda\mu)\nu}^{(3)} T_{(\lambda\mu)\nu}^{(3)}}. \quad (3.26)$$

Reference to a table of results (Table I) enables the symmetry classification of each Raman electro-optically active vibration to be determined on the basis of the value for these two intensity ratios.

Alternatively, a visually more comprehensible diagrammatic method can be employed. Noting the allowed numerical ranges of δ_1 and δ_2 for each class of transition and plotting δ_1 against δ_2 one obtains Fig. 4. For any EFIR transition the point (δ_1, δ_2) , must lie within the triangle XYZ having vertices $(1.9, 6.6)$, $(0, 9.1)$, and $(0, 5.1)$. If the point (δ_1, δ_2) lies on one of the vertices X , Y , or Z , then the transition contains contributions from one weight only and belongs to either class IIB, IV, or III, respectively. If the point lies on one of the sides of XYZ then the transition contains contributions from two weights. For example, a point lying on the line YZ corresponds to a transition which has contributions from weights -2 and -3 only, and thus belongs to class IIA. For a point which lies on XZ the transition has contributions from weights -1 and -3 only, and so belongs to class IB. If the point lies entirely *within* XYZ then the transition contains contributions from all weights and is consequently a class IA transition.

IV. DISCUSSION

It is both useful and necessary to consider the likely magnitude of the electric-field-induced Raman effect. In view of the similarity between the electro-optical Raman scattering tensor T_{ijk} and the hyper-Raman scattering tensor β_{ijk} it is fruitful to compare the intensities of the two effects. If I_{EFIR} represents the intensity of a Raman transition via the electro-optical route and I_{HR} the typical intensity of a hyper-Raman transition then, neglecting the frequency-dependence of the scattering tensors, it can be shown that

$$I_{\text{EFIR}}/I_{\text{HR}} \approx 2c\epsilon_0 E^2 / Ig^{(2)}. \quad (4.1)$$

In Eq. (4.1), $g^{(2)}$ is the degree of second-order coherence of the incident radiation, which for laser light is generally close to unity. For a pulsed laser irradiance of 10^{13} W m^{-2} , and an experimentally feasible electric field strength of $5 \times 10^7 \text{ V m}^{-1}$, the ratio defined in Eq. (4.1) is approximately unity. In fact Lippitsch^{10,14} has shown that by pulsing, external electric field strengths of 10^8 V m^{-1} can be achieved. By careful choice of solvent, *local* electric fields can be significantly higher. Water, for example, gives rise to local electric fields 25 times as large as the external field. Thus in practice electric fields of over 10^9 V m^{-1} can be achieved, which would lead to electro-optical Raman effects 100 times more intense than hyper-Raman scattering.

As Plieth⁵ has shown, similar electric field strengths exist near an electrode within the electrochemical double layer,

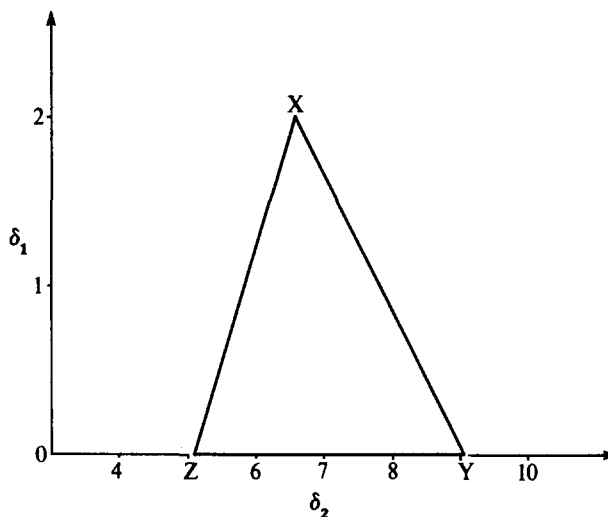


FIG. 4. Symmetry assignment of electric-field-induced Raman transitions in circularly polarized light experiments using the intensity ratios δ_1 and δ_2 .

even in the absence of an applied potential. Studies at metal surfaces must therefore consider the effects of the electric field. In the presence of ionic fluids, diffusion processes may result in the local electric field changing with the distance from the electrode. For spherical ions, the electric field at a distance x from a planar electrode held at a potential ϕ_0 can be calculated using Guoy–Chapman theory, giving the result²⁵:

$$E(x) = \{8kTn^0/\epsilon_0 K\}^{-1/2} \times \sinh\{\ln[(1 + we^{-px})/(1 - we^{-px})]\}, \quad (4.2)$$

where

$$w = \tanh(Ze\phi_0/4kT) \quad (4.3)$$

and

$$p = (2n^0 Z^2 e^2 / K\epsilon_0 kT)^{1/2}. \quad (4.4)$$

In the above equations n^0 is the bulk concentration of the ionic compound, Ze is the charge on the ion, and K is the dielectric constant.

Recently, DiLella *et al.*²⁶ have reported the breakdown of normal Raman selection rules close to, and at, metal surfaces, attributing this to quadrupolar effects due to the highly inhomogeneous electric fields. However, our calculations show that the electric fields experienced by molecules close to metal surfaces are sufficient to give rise to observable electro-optical phenomena, so resulting in a breakdown of the normal Raman selection rules even in the electric-dipole approximation. While quadrupolar effects are strongly in-

TABLE I. Values of the polarization ratios δ_1 and δ_2 for transitions belonging to each symmetry class.

Class weights	IA 1,2,3	IIA 2,3	IB 1,3	IIB 3	IV 2	III 1
δ_1	$1.8 > \delta_1 > 0$	0	$1.8 > \delta_1 > 0$	0	0	1.8
δ_2	$9.1 > \delta_2 > 5.1$	$9.1 > \delta_2 > 5.1$	$6.6 > \delta_2 > 5.1$	5.1	9.1	6.6

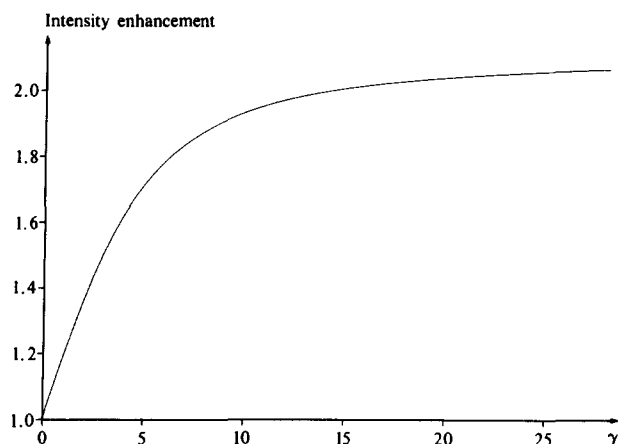


FIG. 5. Enhancement of intensity for a pure weight-0 transition as a function of $\gamma = \mu^{00} E_{\text{mol}} / kT$.

fluenced by surface roughness, the electro-optical dipole channel should be operative at all metal surfaces, and thus represents a more universal mechanism for the breakdown of selection rules at metal surfaces. Furthermore at these field strengths there will be appreciable electrical polarization of the medium. As Lippitsch and co-workers have shown, this can lead to intensity enhancements of 2–3. This is in good agreement with our results, where we have shown that the leading correction to the Raman intensity at these high field strengths can easily be three times the normal isotropic contribution. Figure 5 shows how the intensity of the

component, $\alpha_{\lambda\mu}^{(0)} \alpha_{\lambda\mu}^{(0)}$, varies with field strength for 90° Raman scattering.

In conclusion, our studies have shown that strong static electric fields exert a considerable effect on the Raman spectra of fluids, both in modifying the relative intensities of lines normally present, and by inducing normally Raman-inactive transitions. Our results should facilitate the analysis of EFIR spectra, and hopefully stimulate further experimental studies in this area.

ACKNOWLEDGMENT

N. P. B. gratefully acknowledges financial support from the Science and Engineering Research Council.

APPENDIX A: GENERAL INTENSITY EQUATIONS FOR RAMAN SCATTERING IN ELECTRICALLY POLARIZED MEDIA

The result takes the form expressed by Eq. (2.9) of the main text, where for linearly polarized light the rate cointegrators, A , B , and C are given by the following equations:

$$A = 1/30 \left[\begin{pmatrix} \mathbf{e} \cdot \mathbf{e}' \end{pmatrix}^2 \right]^T \begin{bmatrix} 10 & -1 \\ 0 & 3 \end{bmatrix} \begin{bmatrix} \alpha_{(\lambda\mu)}^{(0)} \alpha_{(\lambda\mu)}^{(0)} \\ \alpha_{(\lambda\mu)}^{(2)} \alpha_{(\lambda\mu)}^{(2)} \end{bmatrix}, \quad (\text{A1})$$

$$B = -1/14 \left[\begin{pmatrix} (\mathbf{e} \cdot \mathbf{e}') \{ (\mathbf{E} \cdot \mathbf{e}) (\mathbf{E} \cdot \mathbf{e}') - (1/3) (\mathbf{e} \cdot \mathbf{e}') \} \\ (\mathbf{E} \cdot \mathbf{e})^2 - (1/3) \\ (\mathbf{E} \cdot \mathbf{e})^2 - (1/3) \end{pmatrix} \right]^T \begin{bmatrix} 18 & -6 \\ -6 & 9 \\ -6 & 9 \end{bmatrix} \begin{bmatrix} \hat{\mu}_v \hat{\mu}_o \{ \alpha_{(\lambda\lambda)}^{(0)} \alpha_{(vo)}^{(0)} + \alpha_{(\lambda\lambda)}^{(0)} \alpha_{(vo)}^{(2)} \} \\ - \alpha_{(\lambda\mu)}^{(0)} \alpha_{(\lambda\mu)}^{(0)} \\ \hat{\mu}_\mu \hat{\mu}_o \{ \alpha_{(\lambda\mu)}^{(0)} \alpha_{(\lambda o)}^{(0)} + 2 \alpha_{(\lambda\mu)}^{(0)} \alpha_{(\lambda o)}^{(2)} \\ + \alpha_{(\lambda\mu)}^{(2)} \alpha_{(\lambda o)}^{(2)} \} - 1/3 \{ \alpha_{(\lambda\mu)}^{(0)} \alpha_{(\lambda\mu)}^{(0)} \\ + \alpha_{(\lambda\mu)}^{(2)} \alpha_{(\lambda\mu)}^{(2)} \} \end{bmatrix}, \quad (\text{A2})$$

$$C = (1/392) [(\mathbf{E} \cdot \mathbf{e})^2 (\mathbf{E} \cdot \mathbf{e}')^2 - (1/7) (4 (\mathbf{e} \cdot \mathbf{e}') (\mathbf{E} \cdot \mathbf{e}) (\mathbf{E} \cdot \mathbf{e}') + (\mathbf{E} \cdot \mathbf{e})^2 + (\mathbf{E} \cdot \mathbf{e}')^2 + (1/35) (2 (\mathbf{e} \cdot \mathbf{e}')^2 + 1)] \\ \times [\hat{\mu}_\lambda \hat{\mu}_\mu \hat{\mu}_v \hat{\mu}_o (\alpha_{(\lambda\mu)}^{(0)} \alpha_{(vo)}^{(0)} + 2 \alpha_{(\lambda\mu)}^{(0)} \alpha_{(vo)}^{(2)} + \alpha_{(\lambda\mu)}^{(2)} \alpha_{(vo)}^{(2)}) - (1/7) [4 \hat{\mu}_\mu \hat{\mu}_o \{ \alpha_{(\lambda\mu)}^{(0)} \alpha_{(\lambda o)}^{(0)} + 2 \alpha_{(\lambda\mu)}^{(0)} \alpha_{(\lambda o)}^{(2)} \\ + \alpha_{(\lambda\mu)}^{(2)} \alpha_{(\lambda o)}^{(2)} \} + 2 \hat{\mu}_v \hat{\mu}_o \{ \alpha_{(\lambda\lambda)}^{(0)} \alpha_{(vo)}^{(0)} + \alpha_{(\lambda\lambda)}^{(0)} \alpha_{(vo)}^{(2)} \}] + (1/35) \{ 5 \alpha_{(\lambda\mu)}^{(0)} \alpha_{(\lambda\mu)}^{(0)} + 2 \alpha_{(\lambda\mu)}^{(2)} \alpha_{(\lambda\mu)}^{(2)} \}]. \quad (\text{A3})$$

APPENDIX B: RAMAN INTENSITIES FOR ELECTRICALLY POLARIZED MEDIA IN SPECIFIC EXPERIMENTAL GEOMETRIES

$$I^{(90;1)}(\parallel \rightarrow \parallel) = K \left[\left[\frac{j_2'}{7} + \frac{j_4'}{56} \right] \alpha_{(\lambda\mu)}^{(0)} \alpha_{(\lambda\mu)}^{(0)} + \left[\frac{1}{10} - \frac{j_2'}{7} + \frac{j_4'}{140} \right] \alpha_{(\lambda\mu)}^{(2)} \alpha_{(\lambda\mu)}^{(2)} \right. \\ + \left[- \frac{2j_2'}{7} - \frac{j_4'}{28} \right] \hat{\mu}_v \hat{\mu}_o \{ \alpha_{(\lambda\lambda)}^{(0)} \alpha_{(vo)}^{(0)} + \alpha_{(\lambda\lambda)}^{(0)} \alpha_{(vo)}^{(2)} \} \\ + \left[\frac{3j_2'}{7} - \frac{j_4'}{14} \right] \hat{\mu}_\mu \hat{\mu}_o \{ \alpha_{(\lambda\mu)}^{(0)} \alpha_{(\lambda o)}^{(0)} + 2 \alpha_{(\lambda\mu)}^{(0)} \alpha_{(\lambda o)}^{(2)} + \alpha_{(\lambda\mu)}^{(2)} \alpha_{(\lambda o)}^{(2)} \} \\ \left. + \frac{j_4'}{8} \hat{\mu}_\lambda \hat{\mu}_\mu \hat{\mu}_v \hat{\mu}_o (\alpha_{(\lambda\mu)}^{(0)} \alpha_{(vo)}^{(0)} + 2 \alpha_{(\lambda\mu)}^{(0)} \alpha_{(vo)}^{(2)} + \alpha_{(\lambda\mu)}^{(2)} \alpha_{(vo)}^{(2)}) \right],$$

$$I^{(90;2)}(\parallel \rightarrow \parallel) = K \left[-\frac{1}{14} [j'_2 + j'_4] \alpha_{(\lambda\mu)}^{(0)} \alpha_{(\lambda\mu)}^{(0)} + \left[\frac{1}{10} + \frac{j'_2}{14} - \frac{j'_4}{35} \right] \alpha_{(\lambda\mu)}^{(2)} \alpha_{(\lambda\mu)}^{(2)} \right. \\ \left. + \left[\frac{j'_2}{7} + \frac{j'_4}{7} \right] \hat{\mu}_v \hat{\mu}_o \{ \alpha_{(\lambda\lambda)}^{(0)} \alpha_{(v o)}^{(0)} + \alpha_{(\lambda\lambda)}^{(0)} \alpha_{(v o)}^{(2)} \} \right. \\ \left. + \left[-\frac{3j'_2}{14} + \frac{2j'_4}{7} \right] \hat{\mu}_\mu \hat{\mu}_o \{ \alpha_{(\lambda\mu)}^{(0)} \alpha_{(\lambda o)}^{(0)} + 2\alpha_{(\lambda\mu)}^{(0)} \alpha_{(\lambda o)}^{(2)} + \alpha_{(\lambda\mu)}^{(2)} \alpha_{(\lambda o)}^{(2)} \} \right. \\ \left. - \frac{j'_4}{2} \hat{\mu}_\lambda \hat{\mu}_\mu \hat{\mu}_v \hat{\mu}_o (\alpha_{(\lambda\mu)}^{(0)} \alpha_{(v o)}^{(0)} + 2\alpha_{(\lambda\mu)}^{(0)} \alpha_{(v o)}^{(2)} + \alpha_{(\lambda\mu)}^{(2)} \alpha_{(v o)}^{(2)}) \right],$$

$$I^{(90;2)}(\perp \rightarrow \perp) = K \left[\left[\frac{1}{3} - \frac{5j'_2}{21} + \frac{3j'_4}{56} \right] \alpha_{(\lambda\mu)}^{(0)} \alpha_{(\lambda\mu)}^{(0)} + \left[\frac{1}{15} - \frac{2j'_2}{21} + \frac{3j'_4}{140} \right] \alpha_{(\lambda\mu)}^{(2)} \alpha_{(\lambda\mu)}^{(2)} \right. \\ \left. + \left[\frac{2j'_2}{7} - \frac{3j'_4}{28} \right] \hat{\mu}_v \hat{\mu}_o \{ \alpha_{(\lambda\lambda)}^{(0)} \alpha_{(v o)}^{(0)} + \alpha_{(\lambda\lambda)}^{(0)} \alpha_{(v o)}^{(2)} \} \right. \\ \left. + \left[\frac{2j'_2}{7} - \frac{3j'_4}{14} \right] \hat{\mu}_\mu \hat{\mu}_o \{ \alpha_{(\lambda\mu)}^{(0)} \alpha_{(\lambda o)}^{(0)} + 2\alpha_{(\lambda\mu)}^{(0)} \alpha_{(\lambda o)}^{(2)} + \alpha_{(\lambda\mu)}^{(2)} \alpha_{(\lambda o)}^{(2)} \} \right. \\ \left. + \frac{3j'_4}{8} \hat{\mu}_\lambda \hat{\mu}_\mu \hat{\mu}_v \hat{\mu}_o [\alpha_{(\lambda\mu)}^{(0)} \alpha_{(v o)}^{(0)} + 2\alpha_{(\lambda\mu)}^{(0)} \alpha_{(v o)}^{(2)} + \alpha_{(\lambda\mu)}^{(2)} \alpha_{(v o)}^{(2)}] \right],$$

$$I^{(35.3;1)}(\parallel \rightarrow \parallel) = K \left[\left[\frac{2}{9} - \frac{j'_2}{9} + \frac{j'_4}{24} \right] \alpha_{(\lambda\mu)}^{(0)} \alpha_{(\lambda\mu)}^{(0)} + \left[\frac{7}{90} - \frac{j'_2}{9} + \frac{j'_4}{60} \right] \alpha_{(\lambda\mu)}^{(2)} \alpha_{(\lambda\mu)}^{(2)} \right. \\ \left. - \frac{j'_4}{12} \hat{\mu}_v \hat{\mu}_o \{ \alpha_{(\lambda\lambda)}^{(0)} \alpha_{(v o)}^{(0)} + \alpha_{(\lambda\lambda)}^{(0)} \alpha_{(v o)}^{(2)} \} \right. \\ \left. + \left[\frac{j'_2}{3} - \frac{j'_4}{6} \right] \hat{\mu}_\mu \hat{\mu}_o \{ \alpha_{(\lambda\mu)}^{(0)} \alpha_{(\lambda o)}^{(0)} + 2\alpha_{(\lambda\mu)}^{(0)} \alpha_{(\lambda o)}^{(2)} + \alpha_{(\lambda\mu)}^{(2)} \alpha_{(\lambda o)}^{(2)} \} \right. \\ \left. + \frac{7j'_4}{24} \hat{\mu}_\lambda \hat{\mu}_\mu \hat{\mu}_v \hat{\mu}_o (\alpha_{(\lambda\mu)}^{(0)} \alpha_{(v o)}^{(0)} + 2\alpha_{(\lambda\mu)}^{(0)} \alpha_{(v o)}^{(2)} + \alpha_{(\lambda\mu)}^{(2)} \alpha_{(v o)}^{(2)}) \right],$$

$$I^{(35.3;2)}(\parallel \rightarrow \parallel) = K \left[\left[\frac{2}{9} + \frac{37j'_2}{126} - \frac{j'_4}{14} \right] \alpha_{(\lambda\mu)}^{(0)} \alpha_{(\lambda\mu)}^{(0)} + \left[\frac{7}{90} + \frac{19j'_2}{126} - \frac{j'_4}{14} \right] \alpha_{(\lambda\mu)}^{(2)} \alpha_{(\lambda\mu)}^{(2)} \right. \\ \left. + \left[-\frac{j'_2}{7} - \frac{j'_4}{7} \right] \hat{\mu}_v \hat{\mu}_o \{ \alpha_{(\lambda\lambda)}^{(0)} \alpha_{(v o)}^{(0)} + \alpha_{(\lambda\lambda)}^{(0)} \alpha_{(v o)}^{(2)} \} \right. \\ \left. + \left[-\frac{19j'_2}{42} - \frac{2j'_4}{7} \right] \hat{\mu}_\mu \hat{\mu}_o \{ \alpha_{(\lambda\mu)}^{(0)} \alpha_{(\lambda o)}^{(0)} + 2\alpha_{(\lambda\mu)}^{(0)} \alpha_{(\lambda o)}^{(2)} + \alpha_{(\lambda\mu)}^{(2)} \alpha_{(\lambda o)}^{(2)} \} \right. \\ \left. + \frac{j'_4}{2} \hat{\mu}_\lambda \hat{\mu}_\mu \hat{\mu}_v \hat{\mu}_o (\alpha_{(\lambda\mu)}^{(0)} \alpha_{(v o)}^{(0)} + 2\alpha_{(\lambda\mu)}^{(0)} \alpha_{(v o)}^{(2)} + \alpha_{(\lambda\mu)}^{(2)} \alpha_{(v o)}^{(2)}) \right],$$

APPENDIX C: GENERAL INTENSITY EQUATIONS FOR ELECTRO-OPTICALLY INDUCED RAMAN SCATTERING WITH CIRCULARLY POLARIZED LIGHT

$$I^{(1)}(c \rightarrow c) = \frac{1}{2} K \begin{bmatrix} 1 \\ \cos \theta \\ \cos^2 \theta \end{bmatrix}^T \begin{bmatrix} -21 & -56 & 259 & 259 & 66 \\ 49 & -504 & 616 & 126 & -56 \\ 56 & 224 & -21 & -91 & 6 \end{bmatrix} \begin{bmatrix} T_{(\lambda\mu)v}^{(1\alpha)} T_{(\lambda\mu)v}^{(1\alpha)} \\ T_{(\lambda\mu)v}^{(1\beta,1\gamma)} T_{(\lambda\mu)v}^{(1\alpha)} \\ T_{(\lambda\mu)v}^{(1\beta,1\gamma)} T_{(\lambda\mu)v}^{(1\beta,1\gamma)} \\ T_{(\lambda\mu)v}^{(2)} T_{(\lambda\mu)v}^{(2)} \\ T_{(\lambda\mu)v}^{(3)} T_{(\lambda\mu)v}^{(3)} \end{bmatrix}, \quad (C1)$$

$$I^{(2)}(c \rightarrow c) = \frac{1}{2} K \begin{bmatrix} 1 \\ \cos \theta \\ \cos^2 \theta \end{bmatrix}^T \begin{bmatrix} 126 & 784 & 651 & 770 & 116 \\ 98 & -1008 & 1232 & 252 & -112 \\ 28 & -448 & -168 & -28 & 28 \end{bmatrix} \begin{bmatrix} T_{(\lambda\mu)v}^{(1\alpha)} T_{(\lambda\mu)v}^{(1\alpha)} \\ T_{(\lambda\mu)v}^{(1\beta,1\gamma)} T_{(\lambda\mu)v}^{(1\alpha)} \\ T_{(\lambda\mu)v}^{(1\beta,1\gamma)} T_{(\lambda\mu)v}^{(1\beta,1\gamma)} \\ T_{(\lambda\mu)v}^{(2)} T_{(\lambda\mu)v}^{(2)} \\ T_{(\lambda\mu)v}^{(3)} T_{(\lambda\mu)v}^{(3)} \end{bmatrix}, \quad (C2)$$

$$I^1(c \rightarrow ||) = \frac{1}{2} K \begin{bmatrix} 1 \\ \cos^2 \theta \end{bmatrix}^T \begin{bmatrix} 7 & 168 & 343 & 476 & 52 \\ 112 & 448 & -42 & -182 & 12 \end{bmatrix} \begin{bmatrix} T_{(\lambda\mu)\nu}^{(1\alpha)} T_{(\lambda\mu)\nu}^{(1\alpha)} \\ T_{(\lambda\mu)\nu}^{(1\alpha)} T_{(\lambda\mu)\nu}^{(1\beta,1\gamma)} \\ T_{(\lambda\mu)\nu}^{(1\beta,1\gamma)} T_{(\lambda\mu)\nu}^{(1\beta,1\gamma)} \\ T_{(\lambda\mu)\nu}^{(2)} T_{(\lambda\mu)\nu}^{(2)} \\ T_{(\lambda\mu)\nu}^{(3)} T_{(\lambda\mu)\nu}^{(3)} \end{bmatrix}. \quad (C3)$$

¹R. P. Cooney, M. R. Mahoney, and A. J. McQuillan, in *Advances in Infrared and Raman Spectroscopy*, edited by R. J. H. Clark and R. E. Hester (Heyden, London, 1982), Vol. 9, p. 188.

²*Surface Enhanced Raman Spectroscopy*, edited by R. K. Chang and T. E. Furtak (Plenum, New York, 1982).

³R. K. Chang, Ber. Bunsenges. Phys. Chem. **91**, 296 (1987).

⁴E. S. Reid, R. P. Cooney, P. J. Hendra, and M. Fleischmann, J. Electroanal. Chem. **80**, 405 (1977).

⁵W. J. Plieth in *Nonlinear Behavior of Molecules, Atoms and Ions in Electric, Magnetic or Electromagnetic Fields*, edited by L. Neel (Elsevier, Amsterdam, 1979), p. 251.

⁶D. L. Andrews, N. P. Blake, and K. P. Hopkins, J. Chem. Phys. **88**, 6022 (1988).

⁷G. E. Stedman, Adv. Phys. **34**, 513 (1985).

⁸C. D. Churcher, Mol. Phys. **46**, 621 (1982).

⁹D. L. Andrews and M. J. Harlow, Mol. Phys. **49**, 937 (1983).

¹⁰M. E. Lippitsch, F. R. Aussenegg, and H. M. Noll, in *Proceedings of the Sixth International Conference on Raman Spectroscopy*, edited by E. D. Schmid, R. S. Krishnan, W. Kiefer, and H. W. Schrötter (Heyden, London, 1978), p. 176.

¹¹M. E. Lippitsch, Phys. Lett. A **55**, 199 (1975).

¹²M. E. Lippitsch and F. R. Aussenegg, Acta Phys. Austriaca **42**, 4 (1975).

¹³H. M. Noll and M. E. Lippitsch, Phys. Lett. A **50**, 233 (1974).

¹⁴M. E. Lippitsch, Phys. Lett. A **68**, 194 (1978).

¹⁵H. M. Noll, J. Phys. E **11**, 621 (1978).

¹⁶S. Kielich, Opto-electronics **2**, 5 (1970).

¹⁷D. L. Andrews and N. P. Blake, Chem. Phys. (in press).

¹⁸I.-C. Khoo, R. R. Michael, and P. Y. Yan, IEEE J. Quantum Electron. **23**, 267 (1987).

¹⁹D. L. Andrews and T. Thirunamachandran, J. Chem. Phys. **67**, 5026 (1977).

²⁰D. L. Andrews and M. J. Harlow, Phys. Rev. A **29**, 2796 (1984).

²¹D. P. Craig and T. Thirunamachandran, *Molecular Quantum Electrodynamics* (Academic, London, 1984).

²²J. A. Koningstein, *Introduction to the Theory of the Raman Effect* (Reidel, Dordrecht, 1972).

²³D. L. Andrews and K. P. Hopkins, J. Chem. Phys. **88**, 6030 (1988).

²⁴G. Placzek and E. Teller, Z. Phys. **83**, 209 (1938).

²⁵B. F. Faulkner and A. J. Bard, *Electro-chemical Methods—Fundamentals and Applications* (Wiley, New York, 1983).

²⁶D. P. DiLella, J.-S. Suh, and M. Moskovits, in *Raman Spectroscopy, Linear and Nonlinear*, edited by J. Luscombe and P. V. Huang (Wiley, Chichester, 1982), p. 63.